

1 Supplementary material for LHCb-PAPER-2017-028

2 This document contains supplementary material that will be posted on the public CDS
3 record but will not appear in the paper.

4 Kinematic ranges

5 In this analysis three rapidity ranges are studied

- 6 • $2.2 < y^\Upsilon < 3.0, p_T^\Upsilon < 20 \text{ GeV}/c,$
- 7 • $3.0 < y^\Upsilon < 3.5, p_T^\Upsilon < 20 \text{ GeV}/c,$
- 8 • $3.5 < y^\Upsilon < 4.5, p_T^\Upsilon < 20 \text{ GeV}/c,$

9 as well as one wide rapidity range $2.2 < y^\Upsilon < 4.5,$ extended to $p_T^\Upsilon < 30 \text{ GeV}/c.$ Comparison
10 of these four kinematic ranges with those used by the CDF [1] and CMS [2] collaborations
11 is presented in Fig. 1.

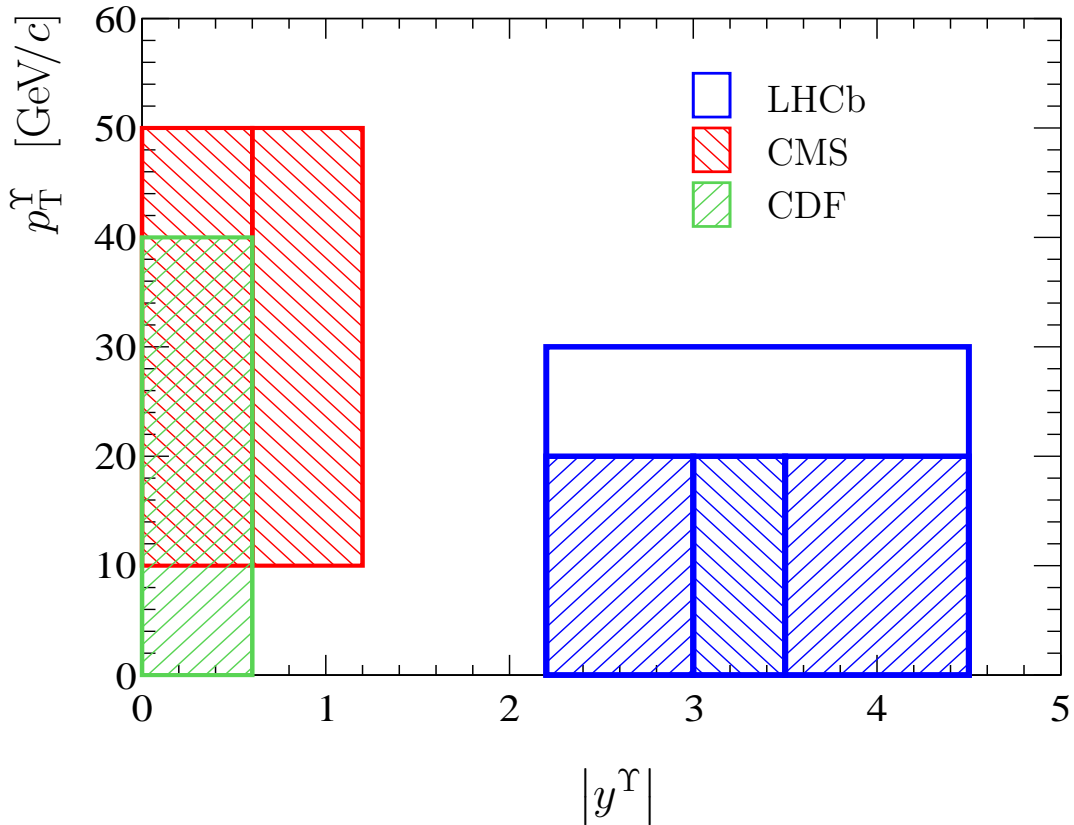


Figure 1: The four kinematic ranges of Υ mesons considered in this analysis in comparison with the kinematic ranges studied by the CDF [1] and CMS [2] collaborations.

12 There is no formal overlap with the previous analyses, but the polarization parameters
13 are expected to have only moderate dependence on $y^\Upsilon,$ allowing a qualitative comparison
14 of results obtained for different $y^\Upsilon.$

15 Comparison with CDF and CMS

16 Comparison with results obtained by the CDF and CMS collaborations are shown in
 17 Figs. 2 and 3 for the HX and CS frames, respectively. The results by the CMS collabo-
 18 ration [2] are obtained in pp collision at $\sqrt{s} = 7$ TeV for the rapidity regions $|y^{\Upsilon}| < 0.6$
 19 and $0.6 < |y^{\Upsilon}| < 1.2$. The results by the CDF collaboration [1] are obtained in $p\bar{p}$ colli-
 20 sion at $\sqrt{s} = 1.96$ TeV for the rapidity region $|y^{\Upsilon}| < 0.6$. There is good agreement with
 21 CMS results for both frames, and with CDF for the CS frame.

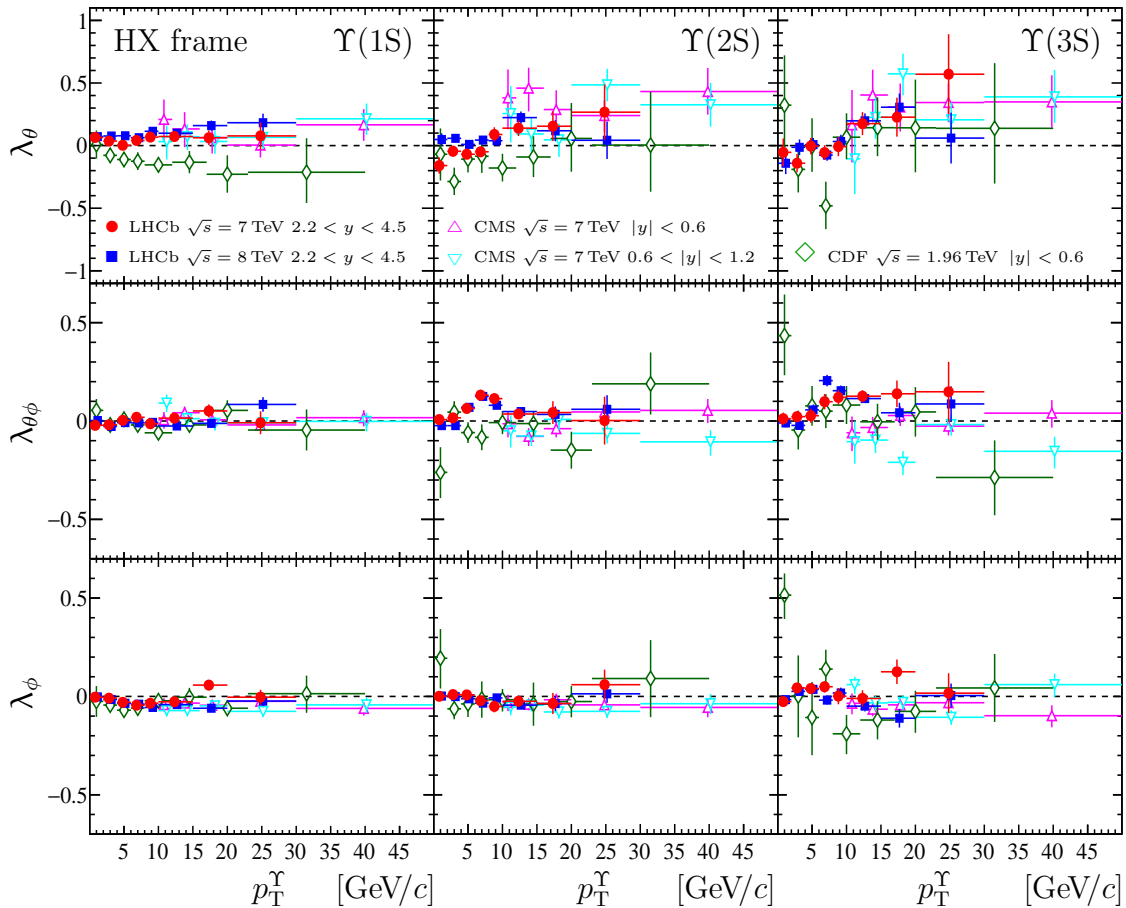


Figure 2: The values of (top) λ_θ , (middle) $\lambda_{\theta\phi}$ and (bottom) λ_ϕ parameters, measured in the HX frame for (left) $\Upsilon(1S)$, (center) $\Upsilon(2S)$ and (right) $\Upsilon(3S)$ mesons. Results of this analysis for the rapidity region $2.2 < y^\Upsilon < 4.5$ are shown with red solid circles and blue solid squares for data collected in pp collisions at $\sqrt{s} = 7$ and 8 TeV, respectively. The results by the CMS collaboration [2] obtained in pp collision at $\sqrt{s} = 7$ TeV for rapidity regions $|y^\Upsilon| < 0.6$ and $0.6 < |y^\Upsilon| < 1.2$ are shown with magenta open upward triangles and cyan open downward triangles, respectively. The results obtained by the CDF collaboration [1] in $p\bar{p}$ collision at $\sqrt{s} = 1.96$ TeV for rapidity region $|y^\Upsilon| < 0.6$ are shown with green open diamonds. Some data points are displaced from the bin centers to improve visibility. The error bars indicate the sum of the statistical and systematic uncertainties added in quadrature.

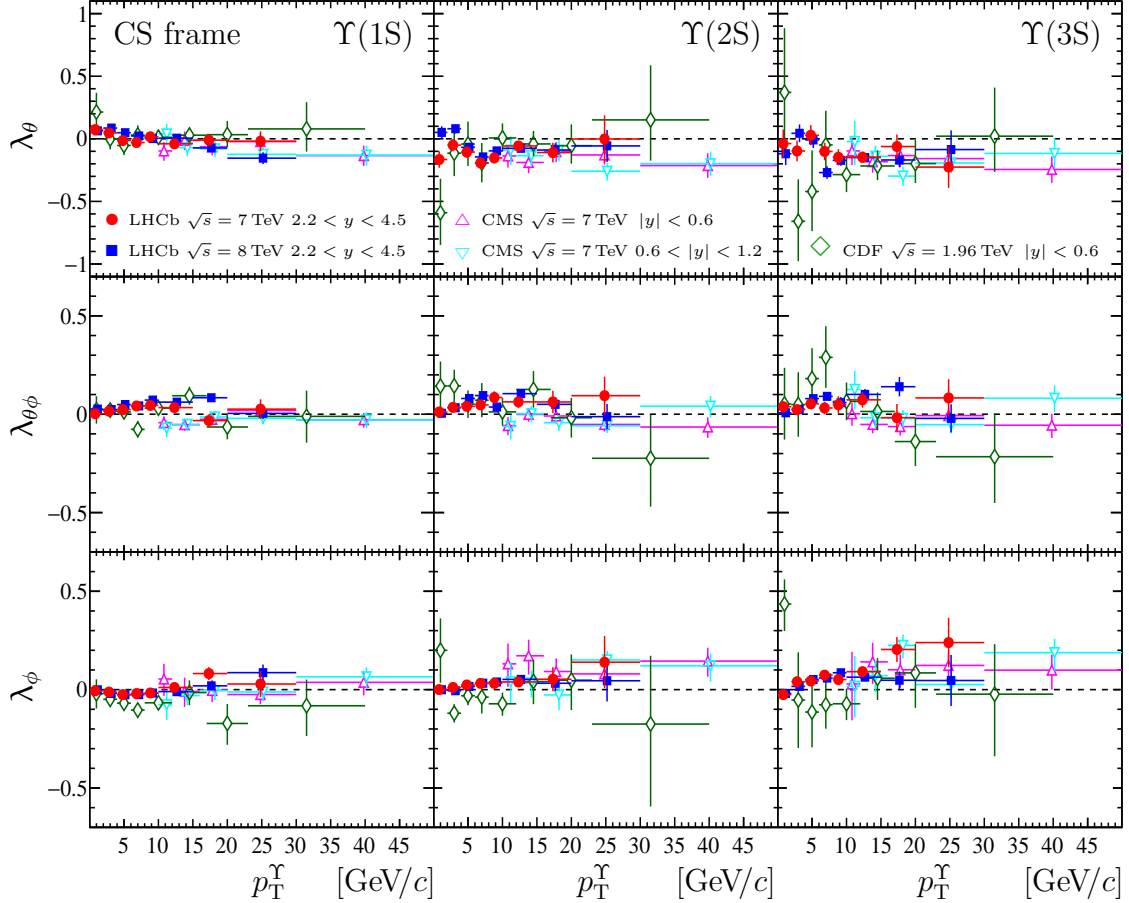


Figure 3: The values of (top) λ_θ , (middle) $\lambda_{\theta\phi}$ and (bottom) λ_ϕ parameters, measured in the CS frame for (left) $\Upsilon(1S)$, (center) $\Upsilon(2S)$ and (right) $\Upsilon(3S)$ mesons. Results of this analysis for the rapidity region $2.2 < y^\Upsilon < 4.5$ are shown with red solid circles and blue solid squares for data collected in pp collisions at $\sqrt{s} = 7$ and 8 TeV, respectively. The results by the CMS collaboration [2] obtained in pp collision at $\sqrt{s} = 7$ TeV for rapidity regions $|y^\Upsilon| < 0.6$ and $0.6 < |y^\Upsilon| < 1.2$ are shown with magenta open upward triangles and cyan open downward triangles, respectively. The results obtained by the CDF collaboration [1] in $p\bar{p}$ collision at $\sqrt{s} = 1.96$ TeV for rapidity region $|y^\Upsilon| < 0.6$ are shown with green open diamonds. Some data points are displaced from the bin centers to improve visibility. The error bars indicate the sum of the statistical and systematic uncertainties added in quadrature.

22 Positivity constraints

23 The parameters λ_θ and λ_ϕ measured for all $(p_T^\Upsilon, y^\Upsilon)$ bins, for data collected at $\sqrt{s} = 7$
 24 and 8 TeV are shown in Fig. 4 together with the regions allowed by the positivity constraints.
 25 The allowed region is shown for the $\lambda_{\theta\phi} = 0$ case. For the case $\lambda_{\theta\phi} \neq 0$ the allowed region
 26 is a bit smaller, but the modifications are proportional to $4\lambda_{\theta\phi}^2$, that is small.

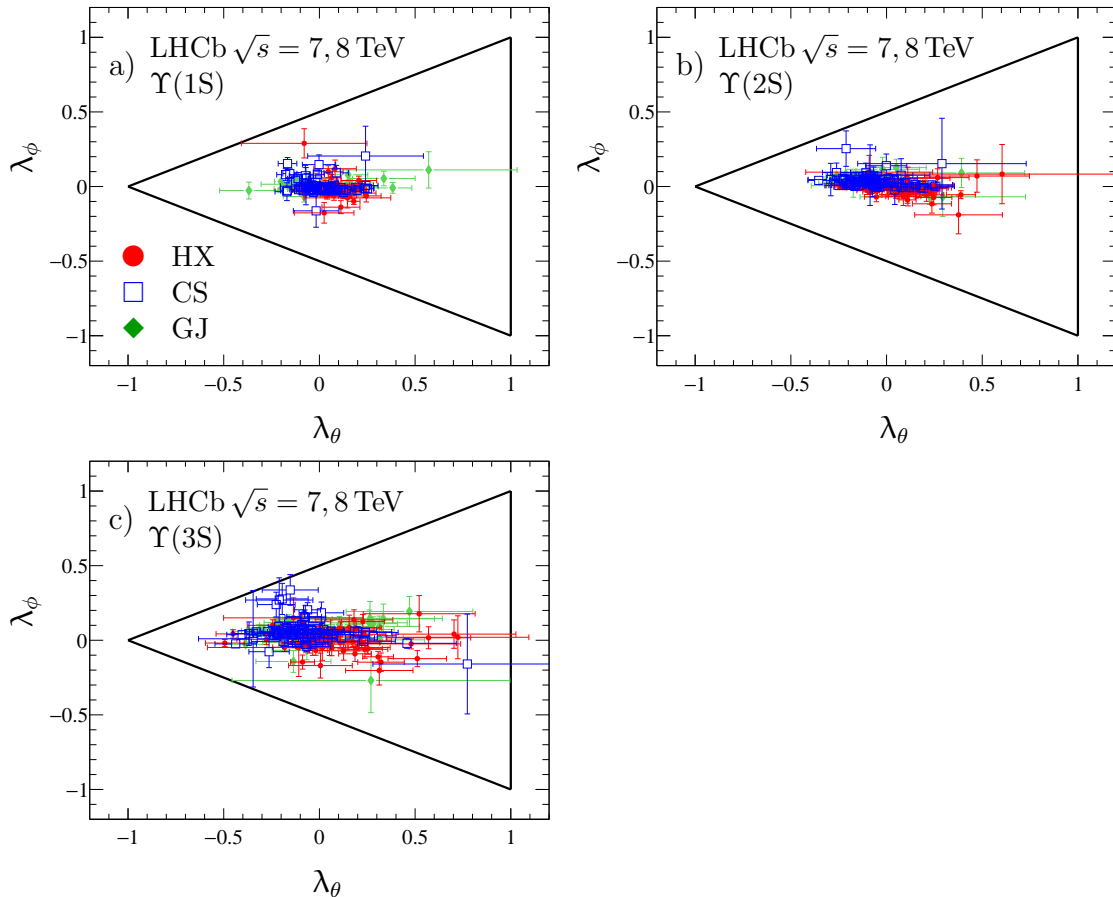


Figure 4: The measured values of $\lambda_\theta, \lambda_\phi$ for a) $\Upsilon(1S)$, b) $\Upsilon(2S)$ and c) $\Upsilon(3S)$ mesons. The red solid circles, blue open squares and green solid diamonds correspond to the helicity (HX), Collins-Soper (CS) and Gottfried-Jackson (GJ) frames, respectively. The thick black lines show the regions allowed by the positivity constraints for the $\lambda_{\theta\phi} = 0$ case.

27 References

- 28 [1] CDF collaboration, T. Aaltonen *et al.*, *Measurements of the angular distributions of*
 29 *muons from Υ decays in $p\bar{p}$ collisions at $\sqrt{s} = 1.96$ TeV*, Phys. Rev. Lett. **108** (2012)
 30 151802, [arXiv:1112.1591](#).
- 31 [2] CMS collaboration, S. Chatrchyan *et al.*, *Measurement of the $\Upsilon(1S)$, $\Upsilon(2S)$ and $\Upsilon(3S)$*
 32 *polarizations in pp collisions at $\sqrt{s} = 7$ TeV*, Phys. Rev. Lett. **110** (2013) 081802,
 33 [arXiv:1209.2922](#).